

ANOMALOUS X-RAY REFLECTIVITY DETERMINES ION-SPECIFIC PROFILE AT MEMBRANES

Ions bound to the surfaces of biological membranes can dramatically affect processes and behaviors of molecules located on or near those membranes. Collaborators from Iowa State University's Ames Laboratory, the Institute of Experimental Physics (Leipzig University, Germany), and The Johns Hopkins University developed anomalous x-ray reflectivity techniques to probe, in detail, the distribution of such ions at a surface that mimics a biological membrane, formally called a biomimetic surface. A biological membrane consists of two lipid-protein (a variety of lipids, cholesterol, and proteins) leaflets bound together at the hydrophobic surface of the lipids, exposing the hydrophilic surfaces to the interior and exterior fluids of a cell or an organelle (Fig. 1). In this case, the biomimetic surface was a lipid monomolecular leaflet (Langmuir monolayer) formed at the gas-water (Ba-solution) interface. To investigate these biomimetic membranes, the researchers used a newly commissioned liquid surface diffractometer at the MU-CAT 6-ID beamline at the APS. The synchrotron x-ray beam at this beamline is both highly monochromatic (i.e., very narrow bandwidth) and tunable (variable x-ray energy).

Several related x-ray fluorescence methods had been developed in the past to probe adsorbed ions at solid and liquid interfaces. The researchers of this study employed the anomalous reflectivity to obtain the location and density of the adsorbed ionic layer near a Langmuir monolayer by collecting x-ray reflectivities at different energies at the absorption edge (resonance) of these ions and away from it.

The basic experimental setup for x-ray reflection involves the detection of a highly monochromatic beam that is mirror-

reflected from the biomimetic surface at various angles of incidence. The special diffractometer at the 6-ID beamline enables *in situ* studies of liquid surfaces and monomolecular layers at a liquid interface. A typical reflectivity curve is measured over a relatively narrow range of incident angles (0° to 5° , depending on the x-ray energy). From a measured reflectivity curve, the average electron-density profile of the film across the interface is determined and can be interpreted in terms of molecular arrangements at the surface.

At energies away from any resonance (absorption edge), the electron density corresponds to the total electrons in the film. On the other hand, for x-ray energies at a resonance of a specific ion, heuristically, fewer electrons of these ions contribute to the reflection process; the effective electron-density at the location of these ions is thereby reduced. Figure 2a shows the effective number of electrons for some of the ions present in the film; whereas, for Cl^- and H_2O this number is practically constant, it varies dramatically for Ba ions in the vicinity of a resonance ($E = 5.247$ keV, for instance).

To form a biomimetic surface, the researchers spread DMPA (1,2-dimyristoyl-*sn*-glycero-3-phosphatidic acid) as a monolayer on dilute aqueous barium chloride (BaCl_2) solutions kept inside a Teflon® Langmuir trough. Their objective was to detect if ions from the solution bind to the charged biomimetic surface and to determine the distribution of these ions in relation to the molecular structure. They collected reflectivities at three distinct x-ray beam energies (E , measured in thousands of electron-volts): 5.1, 5.247, and 8.0 keV. The 5.1 and 8.0 levels were away from an absorption edge, while the 5.247 level

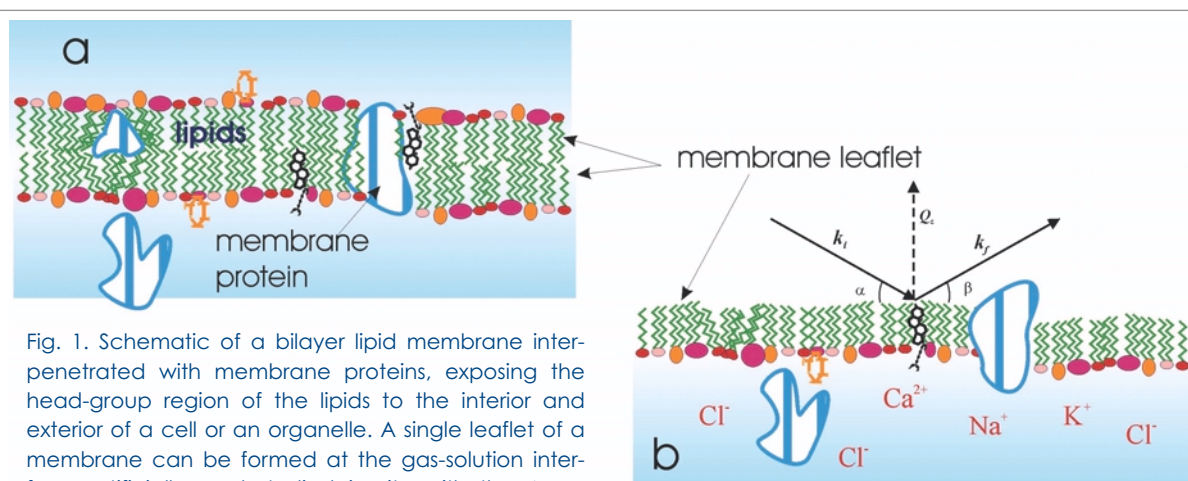


Fig. 1. Schematic of a bilayer lipid membrane interpenetrated with membrane proteins, exposing the head-group region of the lipids to the interior and exterior of a cell or an organelle. A single leaflet of a membrane can be formed at the gas-solution interface artificially, and studied *in situ* with the Ames Laboratory liquid surface diffractometer at the MU-CAT 6-ID beamline. X-ray diffraction from a leaflet system can yield the structure of the film and monitor interfacial phenomena (protein recognition processes, ionic accumulations, and others) relevant to biological processes at membrane surfaces. Note: The above graphic illustrates generic experimental arrangements and does not depict the actual membrane leaflet used in this study. (In this study, only DMPA was present in the membrane leaflet. No membrane proteins were used.)

was located at an absorption edge. Figure 2b shows three reflectivities normalized to the reflectivity of the bare surface water (shifted for clarity). The electron-density (ED) profiles that were determined from those measurements show variations at the head group region of the monolayer, and, from these differences, the distribution and concentration of the Ba ions were extracted. (Ba was chosen to replace Ca, which is abundant in biological solutions, in order to enhance the anomalous scattering effect in this model system study.)

The results pointed to a higher ratio of barium ions present at the surface than would be expected from the stoichiometric ratio alone (i.e., the stoichiometric ratio of 0.5 Ba²⁺ to DMPA⁻). Previously, lower-resolution x-ray research had hinted at the barium ion overabundance on the monomolecular layer. But with the definitive ion profile that anomalous x-ray reflection provided, the researchers in this instance were able to construct a detailed picture of not only the barium ion profile on the Langmuir monolayer, but also the most likely nature of the chemical species at and near that layer. The picture that emerged was one in which the total barium ion distribution was quite asymmetric in nature,

incorporating a bound Stern layer (most likely composed of BaOH⁺ cations) in conjunction with a diffuse cloud of barium cations (Ba²⁺).

Follow-up studies will increase knowledge of the detailed chemistry involved in ion binding to LM layers, including Ca. But this particular research has already demonstrated the power of anomalous x-ray reflection to yield a detailed profile of ion distribution at surfaces. With that profile, detailed chemical information about the surface layer can subsequently be deduced. ○

See: D. Vaknin¹, P. Krüger², and M. Lösche^{2,3}, "Anomalous X-ray Reflectivity Characterization of Ion Distribution at Biomimetic Membranes," *Phys. Rev. Lett.* **90**, 178102-1 to 178102-4 (2 May 2003).

Author affiliations: ¹Iowa State University, ²Leipzig University, ³The Johns Hopkins University

Use of the Advanced Photon Source was supported by the U.S. Department of Energy, Office of Science, Office of Basic Energy Sciences, under Contract No. W-31-109-Eng-38.

ZINC ENZYME CAUGHT IN THE ACT OF CATALYSIS

New x-ray spectroscopy data is helping to resolve a 20-year debate on the catalytic mechanism of a common zinc-containing metabolic enzyme. A group performed the first millisecond-resolution x-ray absorption study on a biological reaction to investigate the way alcohol dehydrogenase removes hydrogen from alcohols. The results suggest that the zinc atom forms two different catalytic intermediates.

Alcohol dehydrogenase (ADH) removes two hydrogen atoms from one of an alcohol's carbon atoms, turning the molecule into an aldehyde or ketone (which contain a carbon-oxygen double bond). Researchers have proposed two basic mechanisms for hydrogen removal. In the traditional mechanism, the alcohol displaces a water molecule bound to a zinc atom, which serves primarily to orient the alcohol. In the alternative scenario, the water molecule stays bound to zinc during catalysis and serves as a temporary site for hydrogen transfer. A key feature distinguishing the two mechanisms is the number

of atoms zinc is bound to—four if water is displaced; five if not. Researchers have had a tough time figuring out what zinc is doing, however, in part because it resists analysis by conventional forms of spectroscopy.

One way of scanning ADH (and other metal-containing proteins) is to bombard it with x-rays that vary in frequency over time and measure the resulting fluorescence spectrum, which provides information on bond length and number of atoms near zinc and is sensitive to zinc's charge and bonding geometry. Varying the x-ray frequency usually takes 50 milliseconds (ms) or longer, however, while the ADH reaction itself takes less than 100 ms. Now a group from the Weizmann Institute of Science in Rehovot, Israel, and Yeshiva University in New York has improved two methods well enough to get around that obstacle.

In one experiment, performed on the National Synchrotron Light Source beamline X9B at Brookhaven National Laboratory, they successively froze the reaction in its tracks to observe it at

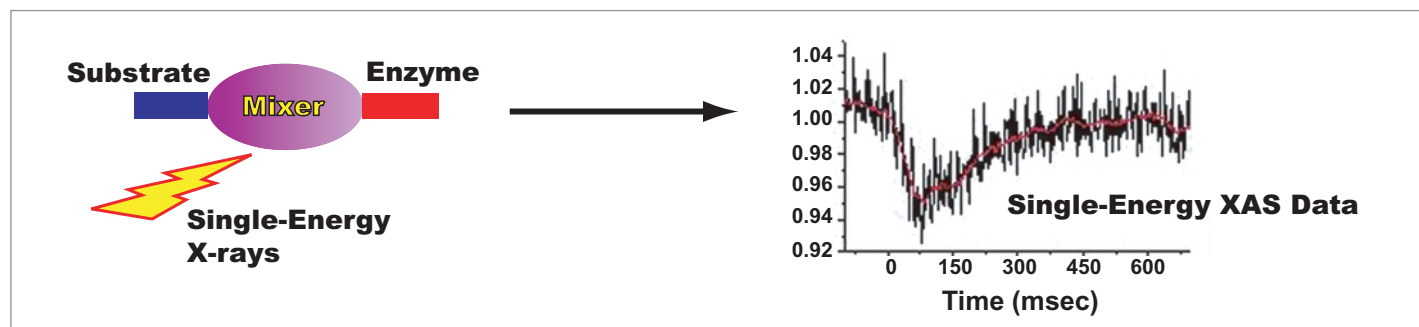


Fig. 1. Kinetic x-ray absorption spectroscopy experiments are used to follow real-time electronic changes, which are related to the structure of the catalytic site. X-ray fluorescence photons are recorded at single X-ray energy by synchronizing X-ray beam, rapid mixer, and fast data acquisition system.

elapsed times ranging from around 2 ms to 110 ms. Enzyme from bacteria and substrate were rapidly mixed and injected into a bath of liquid isopentane, which halts or “quenches” the reaction. Although the quenched molecules are actually in a mix of states, sophisticated mathematical analysis of the fluorescence data indicated the zinc formed two successive five-bond transition states in the first 70 ms after the reactants came together. They proposed that the first transition state forms when water binds to zinc, which then breaks its bond with the protein and binds to the alcohol, forming the second transition state. Water remains bound until the reaction is finished.

In a second experiment, performed on the Bio-CAT beamline 18-ID at the APS, they measured fluorescence at a single x-ray energy over time, down to the millisecond (see Fig. 1). Changes in absorption at that energy correspond to changes in zinc’s charge. They observed a rapid buildup of partial positive charge on zinc, followed by a slow return to neutrality beginning around 70 ms. They interpret the partial positive charge as a sign of the second five-bond zinc transition state, in which the

attached alcohol pulls zinc’s electrons away from it. Theoretical calculations supported the conclusion.

The result suggests the ADH mechanism is more complicated than previously thought, but further experiments will be needed to test the proposed mechanism, and bacterial ADH may behave differently than the mammalian enzyme. The spectroscopic techniques may also prove useful in analyzing other metal-containing enzymes. ○

See: O. Kleinfeld¹, A. Frenkel², J.M.L. Martin¹, and I. Sagi¹, “Active site electronic structure and dynamics during metalloenzyme catalysis,” *Nat. Struct. Bio.* **10**, 98-103 (1 February 2003).

Author affiliations: ¹The Weizmann Institute of Science, ²Yeshiva University

I.S. was supported by the Israeli Science Foundation. J.M.L.M. was supported by the Minerva Foundation. Use of the Advanced Photon Source was supported by the U.S. Department of Energy, Office of Science, Office of Basic Energy Sciences, under Contract No. W-31-109-Eng-38.

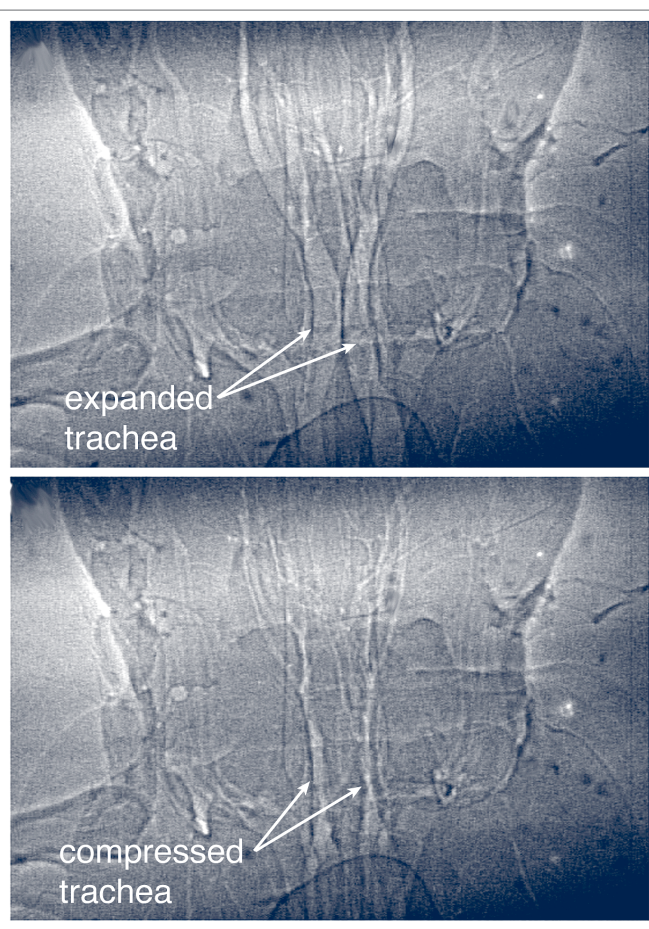
STUDIES OF INSECT RESPIRATION USING PHASE-ENHANCED, TIME-RESOLVED X-RAY IMAGING

Many types of bugs breathe in much the same way that we do. This surprising discovery was made by scientists from Chicago’s Field Museum of Natural History and Argonne National Laboratory, who studied living, breathing insects at the XOR 1-ID beamline of the APS. The investigation revealed the existence of a previously unknown breathing mechanism that is similar to the inflation and deflation of lungs in vertebrate animals.

Scientists had long known that bugs breathe by means of a complex network of gas-filled tubes, called tracheae, that carry oxygen to various parts of their bodies, but it was felt that breathing took place mainly through passive gas diffusion or through changes in internal pressure produced by body motion or hemolymph circulation. The breakthrough came as a result of the ability to take high-resolution x-ray videos of the internal workings of insects in real time as they breathed.

The researchers employed phase-enhanced, time-resolved x-ray imaging, which was enabled by the high flux and partial coherence of the x-ray beams at the APS. The technique produced edge enhancement of the images, with the APS x-ray beams permitting video rates of 30 frames per second. x-ray videos were recorded for the anterior thorax and head regions of ground beetles (*Platynus decentis*), carpenter ants (*Camponotus pennsylvanicus*), house crickets (*Achaeta domestica*), and other insects.

Fig. 1. Ground beetle tracheal images about 0.5 s apart. Upper image shows beetle tracheal tubes fully expanded; in the lower image, they are fully compressed. (Images: Mark W. Westneat)



The tracheal systems were clearly visible as bright branching patterns on the x-ray videos. The tracheae were seen to be inflated at rest (see Fig. 1). They then became squeezed progressively over the course of 300 to 500 msec and subsequently expanded over a similar time period. The tracheae were compressed primarily in one direction so that the roughly circular cross section of a trachea at rest was compressed into an ellipse. Narrowing of the tracheae was often synchronous throughout the head and thorax regions, but local tracheal compression was also observed. The data indicated interspecies variability in both exhalation-inhalation duration and cycle frequency. The researchers also observed other respiratory mechanisms, such as abdominal pumping, autoventilation, and circulatory fluid motion.

Further development of the x-ray imaging technique used in this study could lead to an increased understanding of the basic principles of mammalian, fish, and insect physiology, which could have important implications for humans and their health care. This is because many aspects of human physiology have their counterparts in lower animal orders. For example, studying how larval fish move their backbones could provide information on human backbones, which may provide clues for treating spinal cord injuries in humans. Likewise, studying the walls of blood vessels in mice and the tiny hearts

in beetles (each beetle has multiple “hearts”) may possibly shed light on how to treat high blood pressure.

The imaging technique itself may have medical applications, as turned out to be true of many imaging advances in the past (magnetic resonance imaging, computed axial tomography, computed tomography). The tool also has the potential for a wide variety of other applications, including detecting and studying cracks, voids, and other boundaries inside optically opaque structures; studying fluid flow in rocks and soils for oil exploration and recovery; and characterizing advanced materials, such as ceramics and fiber-reinforced composites. ○

See: M.W. Westneat¹, O. Betz^{1,2}, R.W. Blob^{1,3}, K. Fezzaa⁴, W. J. Cooper^{1,5}, W.-K. Lee⁴, “Tracheal respiration in insects visualized with synchrotron x-ray imaging,” *Science* **299**, 558-560 (24 January 2003).

Author affiliations: ¹Field Museum of Natural History, ²University of Kiel, ³Clemson University, ⁴Argonne National Laboratory, ⁵The University of Chicago

Use of the APS is supported by the DOE Office of Science, Office of Basic Energy Sciences, under Contract no. W-31-109-Eng-38. This research was also funded by grants ONR N000149910184 and NSF DEB-9815614.

SYNTHESIS AND ANALYSIS OF TiO₂-OLIGONUCLEOTIDE HYBRID NANOPARTICLES

New developments in nanotechnology offer the creation of chemical-biological hybrid nanocomposites, which can be introduced into cells to initiate intracellular processes or biochemical reactions. Researchers from Northwestern University Medical Center and Argonne National Laboratory synthesized TiO₂-oligonucleotide nanocomposites made of DNA oligonucleotides attached to 45-Å TiO₂ nanoparticles and tested them by using the XOR 2-ID-E beamline at the APS. A key benefit of nanocomposites is that they could advance medical biotechnology and open new doors in chemistry and materials sciences.

The research goal was to develop the TiO₂-oligonucleotide nanocomposites into nanodevices that could be introduced into cells and function in vivo and in situ. To accomplish that goal, researchers first determined that the nanocomposites could successfully hybridize with long DNA molecules. One concern was that the nanocomposites would “clump” and not be able to withstand an incubation temperature of 95°C, the temperature required for annealing and polymerase chain reaction (PCR). Using atomic force spectroscopy, researchers visualized a

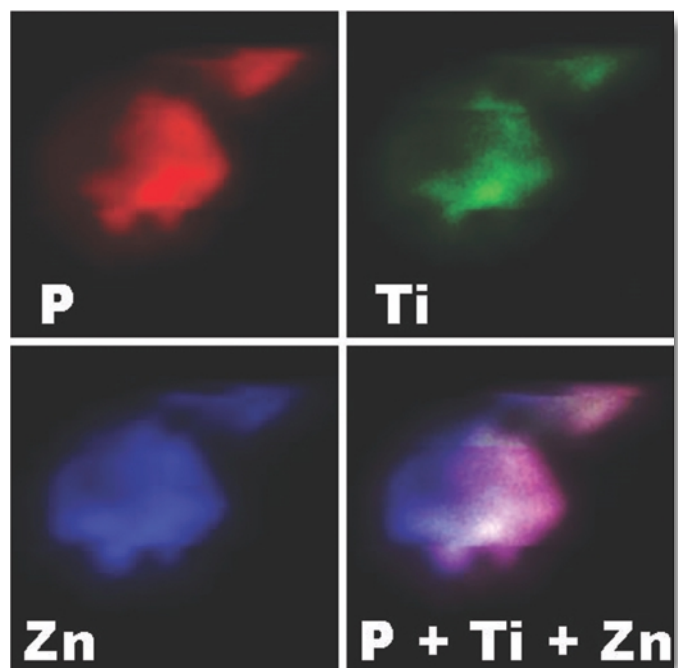


Fig. 1. Scan of a 21 x 21- μm area with a single nucleus containing 3.6×10^6 nanoparticles. Scanning was done in 0.2- μm x 0.2- μm steps, and this nucleus was isolated from cells infected by SuperFect reagent with 80 pmol of R18Ss-TiO₂ hybrid nanocomposite and 160 pmol of “free” R18Ss oligonucleotide, applied onto 4×10^6 cells and incubated for two hours. Nuclei were isolated according to the published procedure. [1] Co-localization of phosphorus (red), titanium (green), and zinc (blue) signals is presented as the overlap of these three colors.

hybridization mixture that had been annealed. The nanocomposite did not clump and withstood the annealing process, paving the way for further research.

Mammalian cells were “infected” in vitro with TiO₂-oligonucleotide nanocomposites by conventional methods. Researchers mapped the location of the titanium in the cells by using titanium-specific K α x-ray fluorescence induced at the APS. In total, researchers used 514 cultured cells from 24 different samples infected with seven different nanocomposites. Depending on the experiment, 20–50% of the cells were found to have accepted and retained titanium nanoparticles. To confirm that the nanocomposites were, indeed, able to enter the cell nucleus, researchers then isolated nuclei from cells infected with a TiO₂ nanocomposite and a “free” oligonucleotide.

Scans revealed titanium in 6 out of 13 sampled nuclei, demonstrating that the TiO₂-DNA nanocomposites reached the nucleus of the mammalian cells. Figure 1 shows that signals of phosphorus and zinc overlap and that the titanium signal showed the highest density in a circular subregion of the nucleus. Given its size and shape, this nuclear subregion is likely to be the nucleolus — the subregion of the interphase nucleus where rDNA is located — and would therefore be the most likely nuclear location for retention of an oligonucleotide-TiO₂ nanocomposite with rDNA sequences attached.

In another experiment, researchers tested the hypothesis that oligonucleotide-TiO₂ nanocomposites are capable of photoinduced endonuclease activity. They showed that DNA oligonucleotides covalently attached to TiO₂ nanoparticles anneal/hybridize to target DNA with specificity dependent on the sequence of the oligonucleotide and participate in PCR reactions. With subsequent illumination, the completed PCR products containing the TiO₂ nanoparticles induced DNA strand breaks in a short distance from the TiO₂.

To gather PCR band cleavage data, researchers used standard PCR reactions. After a reaction, PCR products were

divided equally; white light was then used to illuminate one-half of each reaction for 2 min. Polymerase chain reaction products from non-illuminated and illuminated portions were separated by agarose gel electrophoresis, blotted to Gene-Screen membranes, and hybridized with a radiolabelled probe. Researchers found that, as in the experiments establishing cleavage of oligonucleotides, DNA linked to a TiO₂ nanoparticle did not migrate through the gel. After illumination, however, the same PCR products (primed by the nanocomposite) were cleaved away from the TiO₂ nanoparticle at a random short distance (up to 50 base pairs) and entered the gel, forming a short, diffuse band.

Researchers concluded that even the simple TiO₂-oligonucleotide hybrid nanoparticles synthesized in this project can perform many chemical and biological tasks, including a light-induced site-specific (within 50 nucleotides) nucleic acid endonuclease activity. The nanocomposites analyzed at the APS can perform a multitude of chemical-biological tasks, indicating that other types of TiO₂-biomolecule nanocomposites can be engineered to be nanodevices for medical biotechnology. ○

References

[1] B. Pichon and D. Christophe, *Anal. Biochem.* 261, 233 (1998).

See: T. Paunesku^{1,2}, T. Rajh², G. Wiederrecht², J. Maser², S. Vogt², N. Stojićević^{1,2}, M. Protić², B. Lai², J. Oryhon², M. Thurnauer², and G. Woloschak^{1,2}, *Nat. Mat.* 2, 343-346 (May 2003).

Author affiliations: ¹Northwestern University Medical Center, ²Argonne National Laboratory

T.P., N.S., M.P., J.O. and G.W. were supported by National Institute of Health grants CA81375, CA73042, and NS21442; T.P., T.R., G.W., J.M., S.V., N.S., B.L., M.T., G.W., and use of the APS, were supported by the US Department of Energy, Office of Basic Energy Sciences under contract No. W-31-109-Eng-38.

